Final Report

NASA CR-112108

INVESTIGATION OF FAILURE MECHANISMS IN INTEGRATED VACUUM CIRCUITS

Prepared for:

NATIONAL AERONAUTICS AND SPACE ADMINISTRATION
LANGLEY RESEARCH CENTER
HAMPTON, VIRGINIA 23365

CONTRACT NAS1-10815

STANFORD RESEARCH INSTITUTE
Menlo Park, California 94025 · U.S.A.

STANFORD RESEARCH INSTITUTE
Menlo Park, California 94025 · U.S.A.

Final Report

NASA CR-112108
August 1972

INVESTIGATION OF FAILURE MECHANISMS IN INTEGRATED VACUUM CIRCUITS

By: A. ROSENGREEN

Prepared for:

NATIONAL AERONAUTICS AND SPACE ADMINISTRATION
LANGLEY RESEARCH CENTER
HAMPTON, VIRGINIA 23365

CONTRACT NAS1-10815

SRI Project PYU-1257

Approved by:

PAUL J. JORGENSEN, *Manager*
Ceramics Group

NEVIN K. HIESTER, *Director*
Materials Laboratory
Physical Sciences Division

CHARLES J. COOK, *Executive Director*
Physical Sciences Division

Copy No. 12

ABSTRACT

The fabrication techniques of integrated vacuum circuits are described in detail. Data obtained from a specially designed test circuit are presented. The data show that the emission observed in reverse biased devices is due to cross-talk between the devices and can be eliminated by electrostatic shielding. The lifetime of the cathodes has been improved by proper activation techniques. None of the cathodes on life test has shown any sign of failure after more than 3500 hours. Life tests of triodes show a decline of anode current by a factor of two to three after a few days. The current recovers when the large positive anode voltage (100 V) has been removed for a few hours. It is suggested that this is due to trapped charges in the sapphire substrate. Evidence of the presence of such charges is given, and a model of the charge distribution is presented consistent with the measurements. Solution of the problem associated with the decay of triode current may require proper treatment of the sapphire surface and/or changes in the deposition technique of the thin metal films.

PREFACE

This project was established by the National Aeronautics and Space Administration, Langley Research Center, Hampton, Virginia on May 7, 1971. The NASA project monitor was A. Fripp; A. Rosengreen was project leader at SRI.

CONTENTS

ILLUSTRATIONS

TABLES

I INTRODUCTION

The enormous technical development during the last decade in areas such as space explorations, supersonic transport, and nuclear energy has led to an ever increasing demand for electronic devices and circuits that can operate at high temperatures and/or in environments with high radiation flux densities. In principle, the vacuum tube is the best suited device for operation in such hostile environments, but its use is limited because of its large size and high power requirements. Semiconductor devices, although greatly improved during the last few years, have inherent limitations that prevent them from reaching the same level of radiation hardness as the vacuum tube. With respect to temperature, their limitations are even more severe. Attempts have been made to circumvent these problems by using a large bandgap semiconductor material such as silicon carbide, but the technological problems encountered in growth and processing of this material are so enormous that fabrication of even a diode is difficult.

The Integrated Vacuum Circuit (IVC), a concept developed a few years ago at Stanford Research Institute, may fill the need for a small, radiation hardened, high temperature circuit with a small power consumption per device. It is a marriage of the concept of vacuum tubes with some of the technology used for integrated semiconductor circuits. The principle operation of the device is similar to that of a vacuum tube, but the large three-dimensional electrodes have been replaced by coplanar microminiaturized thin film metal strips on a sapphire substrate. Some of the electrodes are converted to cathodes by coating them with cathode oxides. The entire wafer is heated to about $700^{\circ}C$ in vacuum, allowing electrons from the cathodes to be drawn into the vacuum and collected on the electrodes. Diodes, triodes, tetrodes, and pentodes can be easily fabricated and interconnected, forming

complex circuits of a size limited only by the size of the substrate, cross-talk between the devices, and limitations of the delineation process. Resistors in these circuits are formed by specially designed diodes. Since the entire circuit operates at 700°C and consists of the same materials as a vacuum tube (except for the sapphire, which is a preferred material in radiation hardened circuits)[1] there is good reason to believe that the IVC not only is a high temperature circuit but also has the potential of being a radiation hardened circuit with a hardness close to that of a vacuum tube.

As is usually the case with any device produced by a new combination of separately well-developed technologies and concepts, the birth of the IVC was not without pains. Work performed on a previous contract, NAS 12-607, showed problems with respect to lifetime of the cathodes and the presence of reverse current (emission of electrons from the anode) in some of the devices.[2] The objectives of this project are to study these problems and from this study to evaluate the feasibility and approach of a development program leading to reliable IVCs.

The next section gives the main results and conclusions reached during this program. It is followed by a discussion of the work of the preceding project to provide sufficient background for the technical discussion of the data presented in the last section of this report.

II SUMMARY AND CONCLUSIONS

Two major problems of the IVC, (1) emission from electrode areas other than the cathodes and (2) a short cathode lifetime, have been solved during this program. The emission that appeared as reverse emission from anode to cathode was found to be due to coupling to cathodes of neighboring devices and could be eliminated by proper electrostatic shielding. The lifetime problem was solved by improved activation techniques. So far, none of the cathodes produced during this program has failed after test for several thousand hours, the longest time being in excess of 3500 hours. Both W and a Ni-W alloy, Cathaloy A-31, were used for the backing film of the oxide cathodes with good results. Attempts to replace the less pure grafoil heater strip with strips made from one-mil foils of either Mo or W were not successful, the problem being variation of the thermal contact resistance between heater and substrate. The more ductile Grafoil seems to be superior in this respect.

Life tests on three triodes revealed a reduction in anode current by a factor of two to three after a few days. Removing the anode voltage (approximately 100 V) made the triode recover after a few hours. A similar persistent effect on the anode current was observed when a negative voltage on the order of 10 to 20 V was placed on the shield, but it was significant only at low anode voltages. Measurement with an electrometer showed the existence of a persistent built-in electric field in the sapphire between electrodes, decaying with time constants ranging from minutes to many hours. Models using trapped negative charges in the sapphire at the positive electrodes and positive charges at the negative may explain the observed effects, but because of the complexity of the problem, more study is needed. The effect on the triode current of prolonged applications of

a high voltage on the anode appears to be enhanced by a large surface barrier between the anode metal and the sapphire. Proper treatment of the surface of the substrate may eliminate this problem. The low value of the negative voltage required to obtain a persistent effect on the cathode current may be associated with the fact that this polarity creates negative charge at the cathode that is not neutralized. The effect is not very severe since it is significant only at low anode voltages. The rapid build-up of charges in the substrate may account for the difference between the triode characteristics which consists of a shift along the axis of the anode voltage. Typical values of the amplification factor and the transconductance of the triodes produced from 5-mil-wide electrodes spaced 5 mils apart are 3-4 and 10-12 μ mhos, respectively. No attemps were made to optimize these values.

It is quite obvious from the results of this program that any future program must be directed toward solution of the problem of trapped charges in the substrate. A better understanding is needed not only of the nature of the polarization of the sapphire but also of the flow of electrons in vacuum between the electrodes. This will help the evaluation of the effect of stray electric fields from charges in the substrate and will also provide the tools necessary for evaluation of the effect of the electrode configuration on the device characteristics. The range of values of amplification factor and transconductance that can be obtained using the various device structures should be estimated and evaluated in terms of practical circuits that can be built using those values. Also, estimates should be made of the maximum packing density of circuit elements that can be obtained on the substrate, considering such factors as cross-talk and the area needed for capacitors.

III BACKGROUND

In this section, a brief discussion is given of the structure of the IVC and its problems as they were encountered during a previous contract.[2]

Figure 1 shows a typical pattern of an IVC consisting of four separate one-bit shift registers on a 3/4-inch sapphire wafer. The pattern is formed by delineating the sputtered thin metal films on the wafer by use of photolithographic masking techniques and etching. The main part of the film pattern is made of Mo-Zr alloy, except for the cathodes that consist of a film of pure tungsten covered with cathode oxides. The cathode oxides are deposited by mixing the cathode carbonates with photoresist, applying a thin layer to the wafer and delineating it by use of photolithographic masking techniques. The use of photoresist in the cathode-carbonate mix instead of the normally used butyl binder was found in a previous investigation[3] to have no adverse effect on the thermionic emission. It forms the main basis for the IVC concept since it allows microminiaturization of the cathodes to a degree which heretofore was not possible. The smallest IVC pattern made so far is the one-mil pattern of the four one-bit shift registers shown in Figure 1. Figure 2 shows an enlarged picture of the one-bit shift registers. The width and separation of the electrodes is one mil. The dark areas of Figure 2 are insulating crossover material required in complex patterns for crossing of the metal film conductors. Crossover metal films were not deposited on the circuit shown in Figure 2.

After completion of the IVC pattern, the wafer is mounted in a tube. Figure 3 shows a tube with the upper part of the glass envelope removed.

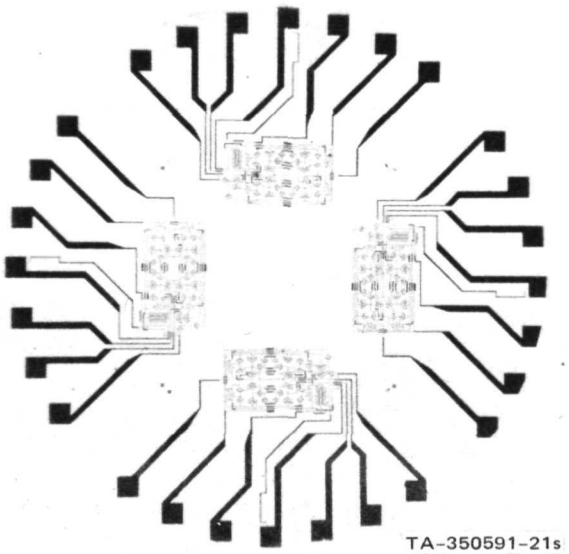

FIGURE 1 FOUR ONE-BIT SHIFT REGISTERS ON A 3/4-INCH SAPPHIRE WAFER

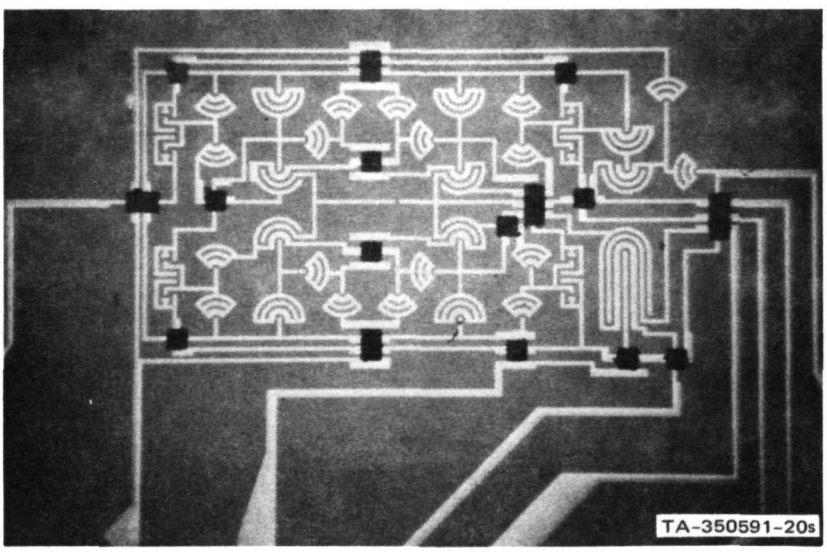

FIGURE 2 ONE-BIT SHIFT REGISTER OF ONE-MIL GEOMETRY. The dark areas are crossover material.

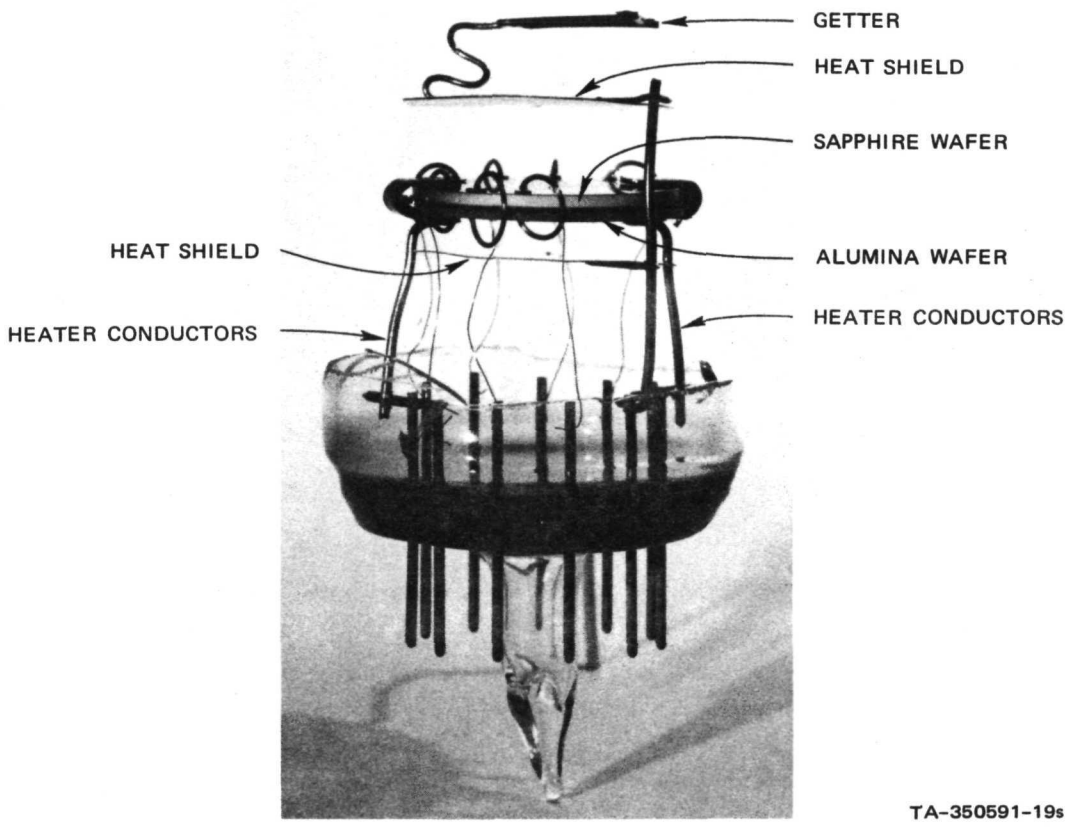

FIGURE 3 MOUNTING OF WAFER IN A TUBE

The sapphire wafer is heated by a strip of Grafoil sandwiched between the sapphire wafer and an alumina wafer. The sandwich is held together by two large clips spotwelded to two nickel supporting rods that also act as conductors for the heater current. To reduce the heat loss from the sandwich, which is heated to 700^{o}C during operation of the IVC, two heat shields are provided, top and bottom. Contacts are made to the circuit by small tungsten clips that touch the small contact pads at the periphery of the sapphire wafer seen in Figure 1. The clips are connected to the pins of the tube header by fine wires. After bakeout the tube is pumped below 10^{-8} torr, the cathodes are activated, and the circuit is ready for use.

The circuit in Figure 1 was tested during the previous contract by dividing it into small sections that by themselves are of practical importance, like the inverter shown in Figures 4 and 5. By testing these simplified circuits it was found that triodes with their anodes connected to a cathode of another device exhibited reverse current; i.e., a current was drawn when the device was reverse biased. At the same time the IVCs proved to have an extremely short lifetime (a few days) because of cathode failure. However, cathodes made from regular cathode sleeves of Ni using the same cathode mix as the IVCs showed no sign of deterioration after more than 10,000 hours. Examination of the failed cathodes indicated that a reaction had taken place on the metal films adjacent to the cathodes. It was speculated that perhaps the tungsten backing film of the cathode was reducing the BaO at too fast a rate, leaving an excess of Ba for evaporation and migration along the connecting metal films. Since Ba is the important material for reduction of the work function necessary for a large thermionic emission of electrons, fast evaporation and migration of a few monolayers of Ba onto the connecting metal films could explain both the short lifetime and the reverse emission. Unfortunately, no time was available to look further into this problem during the last program.

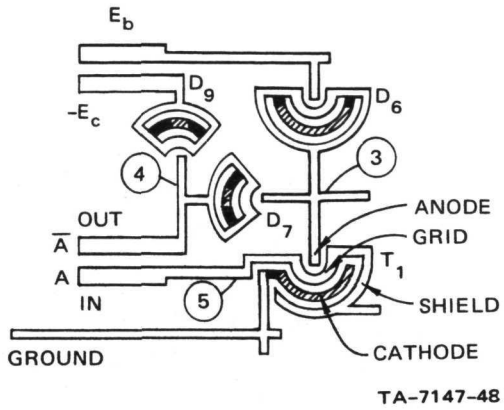

FIGURE 4 LAYOUT OF AN INVERTER

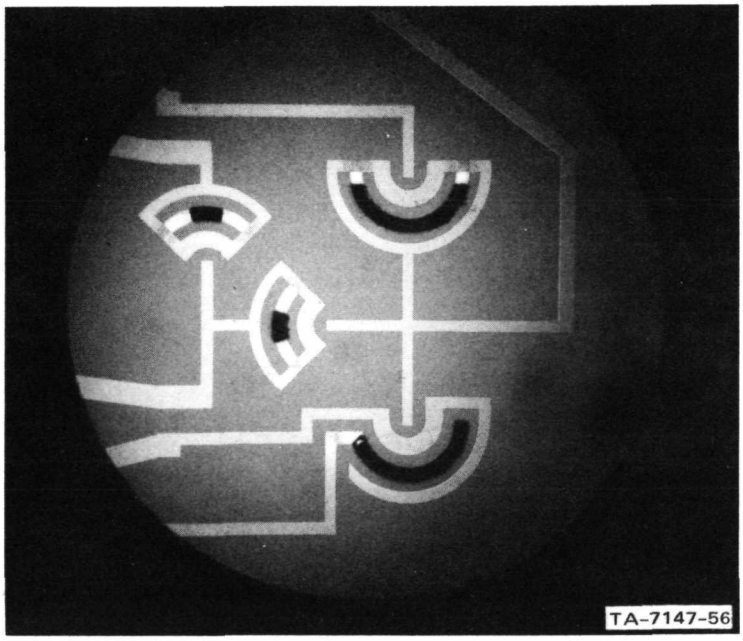

FIGURE 5 PHOTOMICROGRAPH OF AN INVERTER ON A WAFER READY FOR MOUNTING

IV TECHNICAL DISCUSSION

In the following pages we describe the IVC test circuits and the processing required for fabrication of a tube. Selection of the metal for the cathode backing film will be discussed, followed by a presentation and discussion of the results of the measurements on the test circuits.

A. IVC Test Circuit

The IVC test circuit used during this program is shown in Figure 6. It consists of three triodes, A, B, and C, of which two (A and B) are connected in series. The triodes are separated by a common shield. Although it is possible to make the width and the separation of the triode electrodes one mil or less (one-mil geometry was used during the last program), we chose a five-mil geometry so in-house facilities could be used for fabrication of photomasks for delineation of the films.

B. Selection of Metal for Backing Film of Cathodes

The efficiency and life of a cathode in a normal vacuum tube is critically dependent on the chemical interaction between the metal cathode sleeve and the cathode oxides.[4] Selection of the metal for the backing film of the cathodes of the IVCs is therefore of great importance. When the new cathode carbonate mix (using photoresist instead of the normally used butyl binder) was tested originally, the carbonate mix was applied to a nickel sleeve commonly used in the vacuum tube industry. The life test showed no significant deterioration of the thermionic emission after more than 10,000 hours. However, when IVCs were fabricated using tungsten for the cathode backing film failure occurred within a few days, indicating that pure tungsten was perhaps not a good choice.

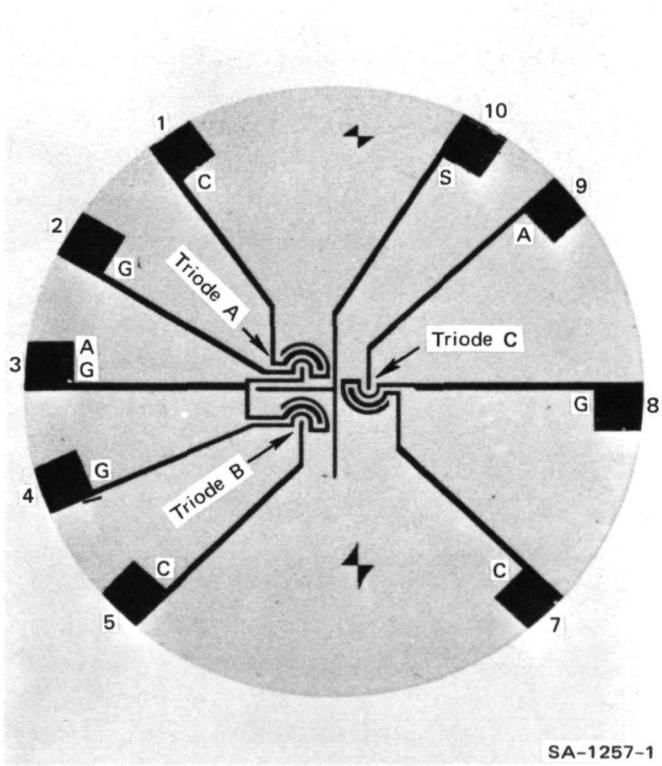

FIGURE 6 IVC TEST CIRCUIT (A: ANODE, C: CATHODE, G: GRID, S: SHIELD)

We have in this program investigated two metals, Pt and a Ni-W alloy, as alternative choices. Pt is often used in vacuum tubes for amplifiers of underwater communication cables where long life is essential.[5] Unfortunately, it is not clear how the activation of the cathode proceeds, since Pt is an inert metal and therefore presumably does not take part in the activation.

The other metal, the Ni-W alloy, is a commonly used material for the cathode sleeve of normal vacuum tubes.[6] A variety of Ni alloys exist for this purpose. We selected an alloy, Cathaloy A-31 from Superior Tube Company, containing approximately 4 wt% W to improve the adhesion of the film to the sapphire substrate. The adhesion of pure Ni to sapphire is usually very poor, while W sticks well to this material. Besides W, the Ni alloy contains a variety of added impurities, some of which are of great importance for the activation and life of the cathode.

In addition to these two metals, the use of W was investigated in more detail, since examination of some of the cathodes from the last program indicated that the use of W for the cathode backing films may not have been the cause of the cathode failure. The color of some of the cathodes was greyish-white, suggesting that not all of the carbon from the photoresist was completely removed, since a well activated cathode is usually pure white. This observation is consistent with the practice used in the last program of completing the activation within a very short period of time.

C. Fabrication of the IVCs

The IVC is commonly fabricated on a 30-mil-thick sapphire disk with a diameter of 0.75 inch. The surface used for the circuit has a 0.2 μ-inch finish, while the other side facing the heater element is provided with a ground finish. Most of the sapphire wafers used were supplied by Insaco, Inc., but a few were delivered by Union Carbide. A few wafers of spinel

($MgAl_2O_4$) from Crystal Technology were also tested to examine the effect of the substrate on the performance of the IVC.

Before deposition of thin films, the wafers went through the following cleaning process: ultrasonic cleaning in alconox and water, rinse in deionized water, immersion in hot water, boiling in hydrogen peroxide, dip in hot distilled water, followed by a 15-minute boiling in deionized water. The wafers were blown dry with cannister Freon gas and fired at 1000°C in air for one hour.

All metal films were approximately 1000 Å thick and were RF sputtered onto the wafers. The entire metal pattern except the cathodes was made from Mo-Zr. The use of Zr was based on the fact that it makes a good bond to sapphire and inhibits the electron emission from any residual cathode oxides left on the films. The Mo-Zr was sputtered from a target of Mo to which small pieces of Zr were attached. The ratio of the area of Mo to Zr was 5:1. The Mo-Zr film was delineated by etching in Aqua Regia for about one-half minute, using a mask of photoresist (KTFR) produced by photolithographic techniques. After etching and removal of the mask, the cathode metal Pt, Ni-W, or W was sputtered onto the wafer and delineated using a new photoresist mask covering only the cathode areas. The etchant being used in the following etching step depended on the cathode metal and was selected so that it did not seriously attack the already delineated Mo-Zr film which was uncovered. The various etching processes that were used are listed in Table I. After each etching process the wafers were rinsed in deionized water, blown dry by Freon gas and baked at 85°C for five minutes. Usually a batch of three to five wafers were processed together.

The photoresist cathode mixture consisted of 71 wt% C-10 triple carbonate mixture* (Sylvania) and 29 wt% KTFR with a little KTFR thinner

*This mixture consists of 57.2% BaO, 38.8% $SrCO_3$ and 4% $CaCO_3$.

added to obtain a viscosity close to that of KTFR. Three drops of the mixture were applied to the wafer with an eyedropper and the wafer was spun at 2000 RPM for 20 seconds. After masking and exposure, all of the photoresist-carbonate mixture was removed except at the cathode areas.

Table I

ETCHING PROCESSES FOR VARIOUS CATHODE METALS

Metal	Etchant	Temperature (^{o}K)	Time (minutes)
Ni-W	HF, HNO_3, H_2O(1:1:3)	300	1/2 to 3
W	HF, HNO_3, H_2O(1:5:5)	300	1/2
Pt	HCL, HNO_3, H_2O(9:1:10)	340	12

D. Assembly of Tubes

The general tube structure was described briefly in Section III above. In this section the assembly and processing of all the parts are described in more detail.

The sandwich (see Figure 3) consisting of a sapphire wafer with circuitry on one of its surfaces, a Grafoil* heater strip, and an alumina wafer (30 mils thick) was held together with two large clips of Mo, each spotwelded to 30-mil Ni wires. The Ni wires were attached to the tungsten pins of the tube header and served as conductors for the heater current. Contacts were made to the circuitry on the sapphire wafer by small tungsten clips connected to the pins of the tube header by five-mil Ni wires. To obtain a more uniform heat distribution, reflectors of Ni were mounted above and below the sandwich. A barium getter was mounted at the top of the tube.

*Carbon Product Division, Union Carbide Corporation, New York, N.Y.

All the metal parts except the precleaned barium getter were cleaned ultrasonically in alconox and water and rinsed in deionized water. After rinsing they were fired in hydrogen, the parts of Mo and Ni at 1000°C for 30 minutes and the tungsten clips at 800°C for ten minutes.

Heater strips were cut from a ten-mil sheet of Grafoil in the same shape as the sapphire wafer. Incisions were made in the Grafoil heater strip to increase the resistance and form a bifilar pattern. Before mounting, the heaters were fired in hydrogen at 1000°C for 30 minutes. The alumina wafer which forms the back part of the sandwich was cleaned similarly to the sapphire wafer, except for the boiling in hydrogen peroxide.

The tube header was made from uranium glass and provided with 11 tungsten pins. Before assembly of the tube, the pins on the inside of the tube were etched electrolytically in a solution made by adding 100 g NaOH and 300 g $NaNO_2$ to 1800 cc H_2O. After etching, the header was cleaned ultrasonically in Alconox, rinsed in deionized water, and dried in hot air from a heat gun. The glass envelope of the tube was made from Nonex glass, Corning Type 7720, which was ultrasonically cleaned in Alconox, rinsed in deionized water, soaked in dilute nitric acid, rinsed again in deionized water, and then dried in hot air. The header and envelope were sealed together on a glass lathe. To prevent oxidation of the inner parts of the tube, a positive pressure of dry nitrogen was applied to the tube during the sealing operation. The tube was attached to a Varian 80 liter/sec VacIon pump provided with a water-cooled titanium sublimation booster and an absorption pump. After roughing, the tube was baked out overnight at 400°C. When the tube had cooled down the getter was degassed, using RF heating, and the titanium booster pump was activated. At a pressure of approximately 10^{-9} torr activation was started.

E. Activation of Cathodes

Before activation can take place, the photoresist must be removed from the cathode carbonates and the carbonates must be converted to oxides. To accomplish this, the substrate was heated rapidly (a few minutes) to about 450°C, at which point the pressure started increasing due to decomposition of the photoresist. To prevent the decomposition gases from lifting the carbonates from the cathode metal film, the rate of temperature increase was reduced to 10 to 20°C/min. Simultaneously with the pressure increase, which usually reached a value of 10^{-8} torr, a large leakage current was observed between grid and cathode of the triodes. The leakage current originated from a voltage of 10 V usually applied between grid and cathode to observe the state of the cathodes during activation. The leakage current increased gradually up to several mA at 700-750°C after which it gradually decreased. At about 850°C the emission current started to dominate and the leakage current fell practically to zero. During the entire heating cycle from 450 to 850°C the pressure stayed in the region of 10^{-8} torr, determined largely by outgassing of the substrate and the Graphite heater and reduction of the carbonates to oxides.

The activation was initiated by heating the substrate to approximately 1050°C. In this process part of the BaO is reduced to Ba which reduces the work function of the oxide mixture. Since the pressure of Ba at these elevated temperatures is relatively high, the duration of the activation process is usually made short to prevent a high loss of Ba by evaporation. In this study the activation was completed after five minutes. The rate of heating was largely determined by the expansion of the substrate and was usually of the order of 100°C/min. Too fast a temperature change resulted in breakage of the substrate due to buildup of stresses at the large Mo clips holding the sandwich together. During activation, the pressure increased to about 10^{-7} torr. The progress of activation was monitored by the emission current between cathode and grid. The current was found

to have a beneficial effect on the cathodes, probably by inducing electrolytic reactions. When increase of the emission current leveled off, the temperature was reduced rapidly to about 700°C and the tube was left with 10V between grid and cathode for 12 hours before measurements were started.

The pressure during the activation was measured close to the VacIon pump. It is estimated that the pressure in the tube was approximately two orders of magnitude higher than the measured value. The temperature was measured optically by use of a commercial detector (Infrascope). To determine the correct setting of the emissivity on the detector, an experiment was performed in which the temperature was measured optically and by use of a thermocouple (two-mil wires) cemented to the sapphire surface. The optics of the detector was adjusted so that it was possible to focus on a very small area of the sapphire substrate, preventing any of the metal films from appearing in the field of view of the detector. The emissivity value at which the two methods gave the same temperature reading at 700°C was 0.6. This value was used during the entire program.

F. Life Tests

The first tubes produced during this program were IVCs with the cathode backing films made of Ni-W. All of these tubes exhibited catastrophic failure after a few days of operation. Closer examination showed that the Ni-W films agglomerated; this is illustrated by the photomicrograph in Figure 7 of a Ni-W film kept at 700°C for two days. The agglomeration eventually led to electric disconnection of the cathodes. The reason for the agglomeration is the high mobility of the Ni atoms at 700°C, which allows the film to reduce its large surface energy by assuming a configuration with a smaller surface to volume ratio. In areas where the surface energy of the Ni-W films was reduced because of a covering layer of cathode oxides no agglomeration took place. Taking advantage of this fact, it was possible to obtain stable tubes by changes in the metalization, as illustrated in Figure 8. Instead of letting the

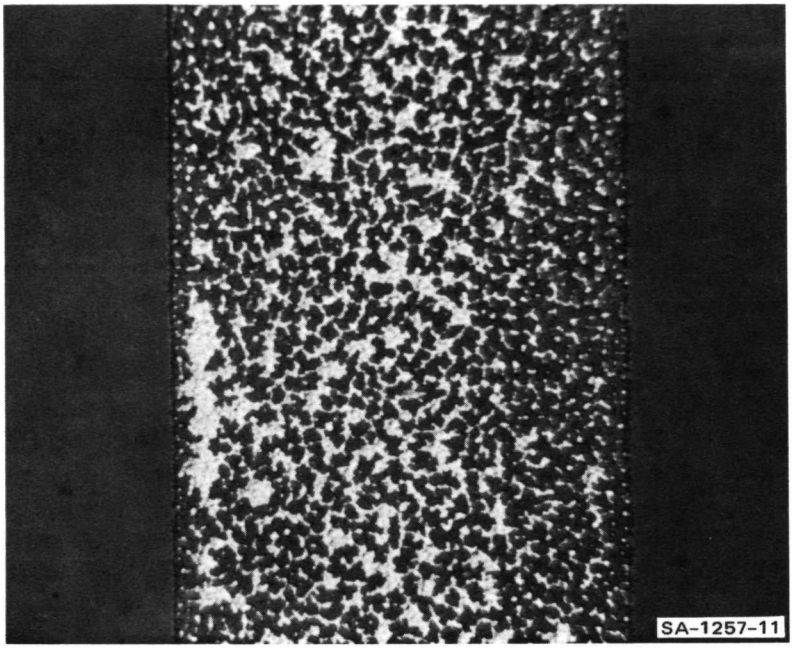

FIGURE 7 PHOTOMICROGRAPH (400X) OF AN AGGLOMERATED Ni-W FILM. The photomicrograph was provided by A. Fripp.

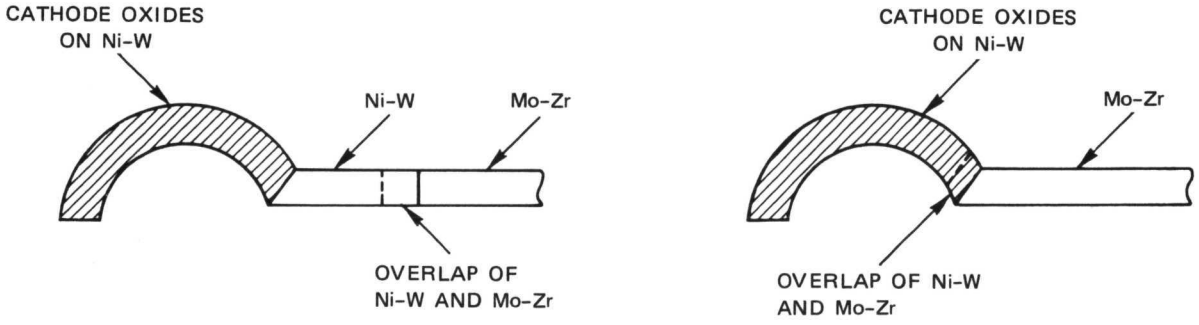

FIGURE 8 CATHODE STRUCTURE

Ni-W and Mo-Zr films overlap a distance away from the cathode, the overlap now occurred underneath the cathode, thus avoiding free surfaces of Ni-W. The overlap of the films underneath the cathodes was made as small as possible to avoid any serious adverse effect on the thermionic emission by Zr diffusing through the Ni-W film and reacting with the cathode oxides.

Table II lists the life test data obtained on different types of cathodes. The data were obtained by measuring the diode current at a constant anode voltage and cathode temperature (700°C). By a diode we are referring to the structure consisting of grid and cathode of a triode. The diodes are labeled A, B, and C according to the triode to which they belong. The diode of tube 1NL is an exception. It is a conventional diode made to check the tube processing. The data of Table II show no indication of cathode failure. The variation of the current is within the accuracy of the test except for tubes 6NL and 8NL, which show a larger increase in current. This may be due to interactions from the substrate, which will be discussed later. The variation of current from diode to diode is relatively large, but significant improvements were obtained later in the program when the procedure of reverse biasing one of the diodes of the test circuit during activation was abandoned. The prodecure was used to distinguish between leakage and emission current during activation, but resulted consistently in poor emission of the diode that had been reverse biased. By forward biasing all diodes at 10 V during the activation, more uniform diode characteristics were obtained.

Contrary to the diodes, the IVC triodes proved to be unstable, as is illustrated in Table III. The current slowly decreased and assumed after a few days of test the values shown in the right hand column of Table III. These currents appear to be steady state values. Only Tube 20NL was left on life test. Its current still remained at 42 μA after 620 hours of test.

Table II

LIFE TEST OF DIODES WITH CATHODE AT 700°C

Tube No.	Diode	Cathode Metal	Anode Voltage (V)	Initial Current (μA)	Duration of Life Test (hours)	Final Current (μA)
1NL		Standard Ni sleeve	13.2	1850	6240	1700
6NL	A	Ni-W film	9.0	40	3650	54
8NL	A	Ni-W film	9.0	8.6	3550	10.8
11NL	B	W-film	9.0	25	2160	24

Table III

LIFE TEST OF TRIODES WITH CATHODE AT 700°C
(Grid and Cathode was Connected to Ground)

Tube No.	Triode	Anode Voltage (V)	Initial Current (μA)	Duration of Life Test (hours)	Final Current (μA)
16NL	B	80	63	72	24
20NL	B	96	78	96	42
21NL	B	97	67	120	24

After removal from life test, diode B of the tubes 16NL and 21NL were investigated further. It was found that the emission of the diodes returned to the original level in a matter of hours. When triode operation was resumed, the emission started to decrease again. Diode B of tube 20NL exhibited a similar behavior, but triode B differed from the other triodes by exhibiting an extremely fast decrease of current. The current fell from 78 μA to about 50 μA in a few minutes. We believe that the reason for these drastic changes is associated with trapped charges in the vicinity of the electrodes when a high voltage ($\approx$ 100 V) is applied to the anode. The effect of trapped charges in the substrate will be discussed in more detail in a later section.

G. Characteristics of Diodes

Figure 9 shows a log-log plot of the current density of the three diodes of tube 21NL as a function of voltage. At low voltages the current is limited by a retarding potential of the order of five to ten volts, too large to be accounted for by the contact potential between cathode and grid. If we assume that the work function of the cathode is close to one eV and that the work function of the Mo-Zr electrode is close to that of Mo, approximately 4 eV, the retarding potential seen by the electrons should be about 3 V. However, since the Mo-Zr film was exposed to the etching solution of Ni-W or W, contamination of the film surface may have changed its work function. Also, polarization and charging of the substrate may have had some effect. At voltages above 10 V the current of all the diodes is space charge limited, characterized by a slope of 3/2. Some variation between the emission of the diodes is observed. It cannot be accounted for by differences in the retarded potential, but is more likely caused by the processing. No attempts were made to "age" the cathodes, a process usually used in commercial tubes to obtain more uniform cathodes.

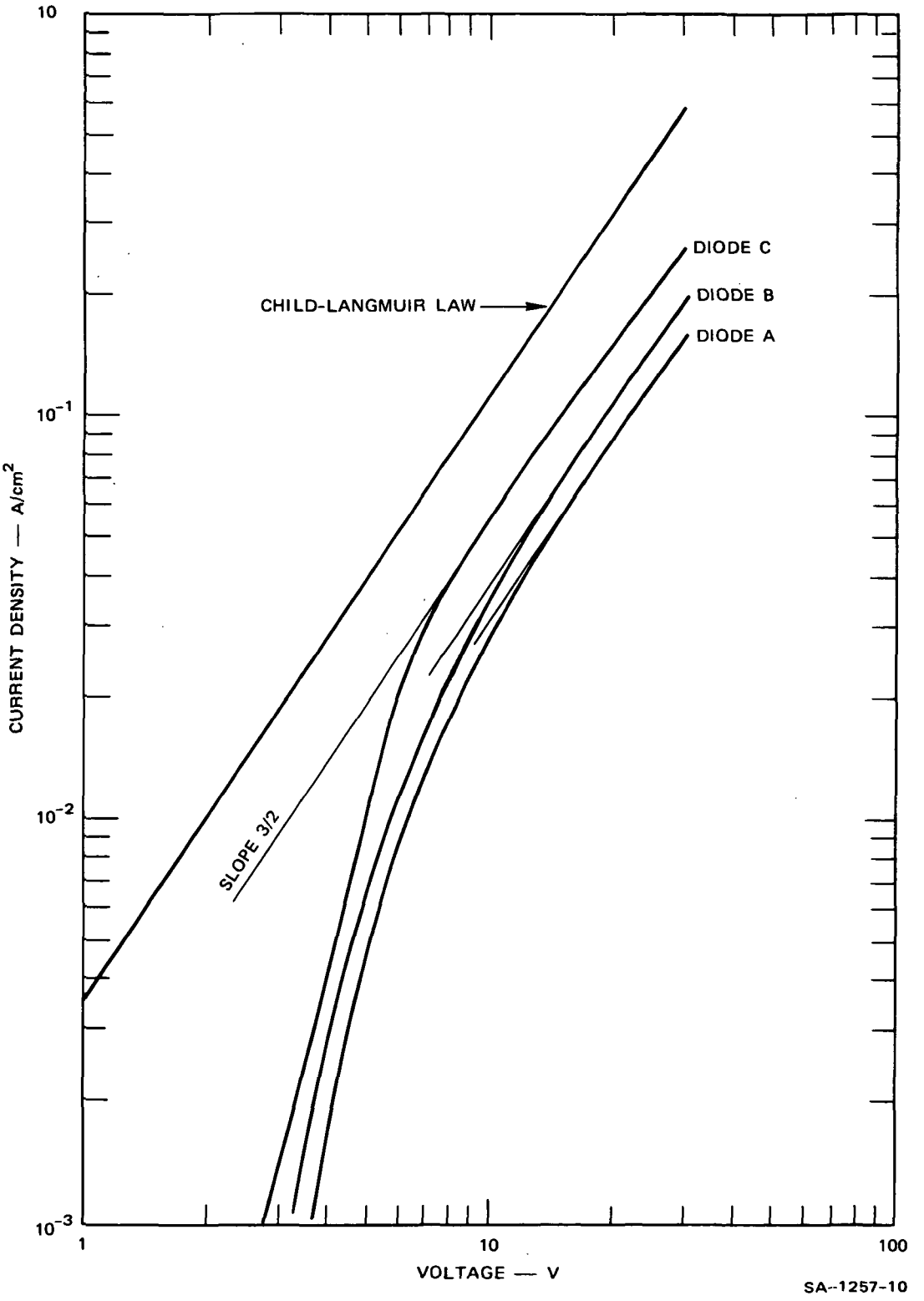

FIGURE 9 CURRENT DENSITY OF THE DIODES OF TUBE 21NL AS A FUNCTION OF VOLTAGE. Also shown is Child-Langmuir Law for a planar diode with 10 mil separation between the electrodes.

Evaluation of the absolute performance of the cathode from the diode characteristics is very difficult. No theoretical expression exists for the current density of a coplanar geometry, and development of such an expression is a research program in itself. To get some idea about the quality of the cathode, we have plotted in Figure 9 the Child-Langmuir Law for a conventional planar diode[7] consisting of two parallel plates. This law states that a current density of J of a planar diode with an electrode separation of d is given by

$$J = 2.335 \times 10^{-6} \frac{V^{3/2}}{d^2} \quad \text{amps/unit area} \qquad (1)$$

when a voltage V is applied between the electrodes. The problem that arises in using this equation on a geometry like the one shown in Figure 10 is the choice of a good value for d. We have chosen the separation between the center of the electrodes (10 mils) as a mean value for d. In comparing the value of J calculated from Eq. (1) with the experimental results, the choice of the effective area of the cathode presents another problem. We have conservatively used the total area of the cathode, although the main part of the current most likely comes from a small area close to the edges of the cathode. Figure 9 shows that the curve of the best diode, diode C, is within a factor of two of the calculated curve in the space charge limited region.

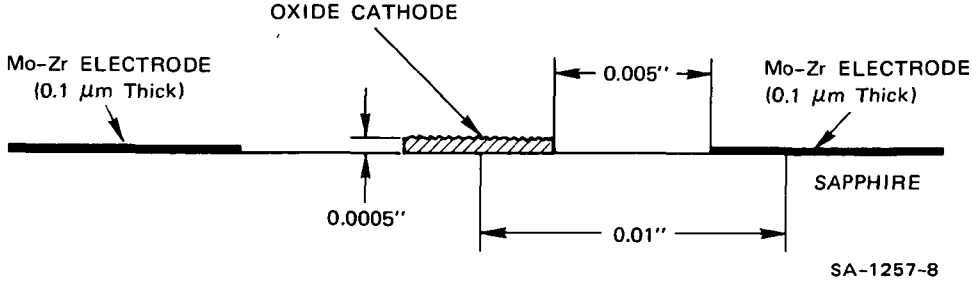

FIGURE 10 STRUCTURE OF COPLANAR DIODE

To obtain more information about the cathodes, attempts were made to measure their saturation current. To prevent damage to the cathodes at the high current densities, the diodes were pulsed with high voltage pulses of a few μs duration at a slow repetition rate. It was necessary to increase the voltage close to 1000 V before there was any sign of saturation. The current density at this level was 4 to 6 A/cm^2, in good agreement with published data on the pulsed saturation current density for oxide cathodes at 700°C.[6] Usually the pulsed saturation current density exceeds the dc value by a factor of ten. However, the voltage required to reach saturation is much too high. If we assume that the average diode current at 10 V is 25 mA/cm^2, the saturation should occur at about 350 V, according to the Child-Langmuir Law; but, as we have seen from the life tests of the triodes, application of high voltages to the electrodes has a temporary adverse effect on the emission and may account for this discrepancy.

The effect of a high anode voltage on the thermionic emission is illustrated in Figure 11, which shows the change of the current density of diode A immediately after measurements of the I-V characteristics of triode A. During this operation, up to 100 V was applied to the anode. Curve "b" is the perturbed characteristic of the diode, which slowly drifted back and assumed that unperturbed position indicated by curve"a". The recovery time was not measured for this particular diode, but in general it was found to vary from minutes to many hours depending on the diode. Also, the magnitude of the change varied from diode to diode. The curves in Fig. 11 show that for this particular diode the effect induced by the high anode voltage is equivalent to an additional retarding potential of approximately 3 V.

H. Characteristics of Triodes

The results presented in this section were obtained from tubes produced after the fabrication techniques of the IVC had been well established. Figure 12 to 16 show some typical triode characteristics. Table IV lists

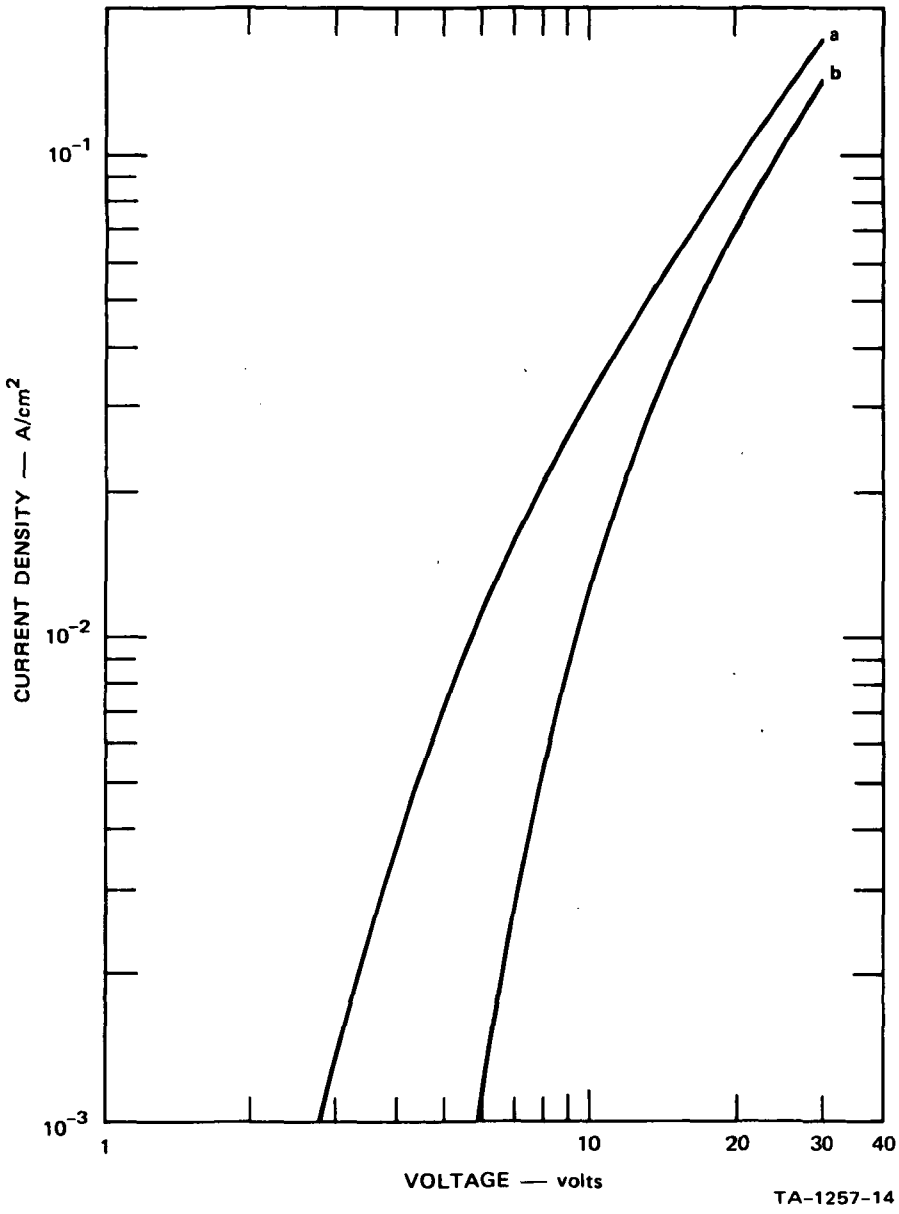

FIGURE 11 V-I CHARACTERISTIC OF DIODE A, TUBE 21NL. Curve a is the original curve. Curve b was measured immediately after triode A had been operated for a short time (hour).

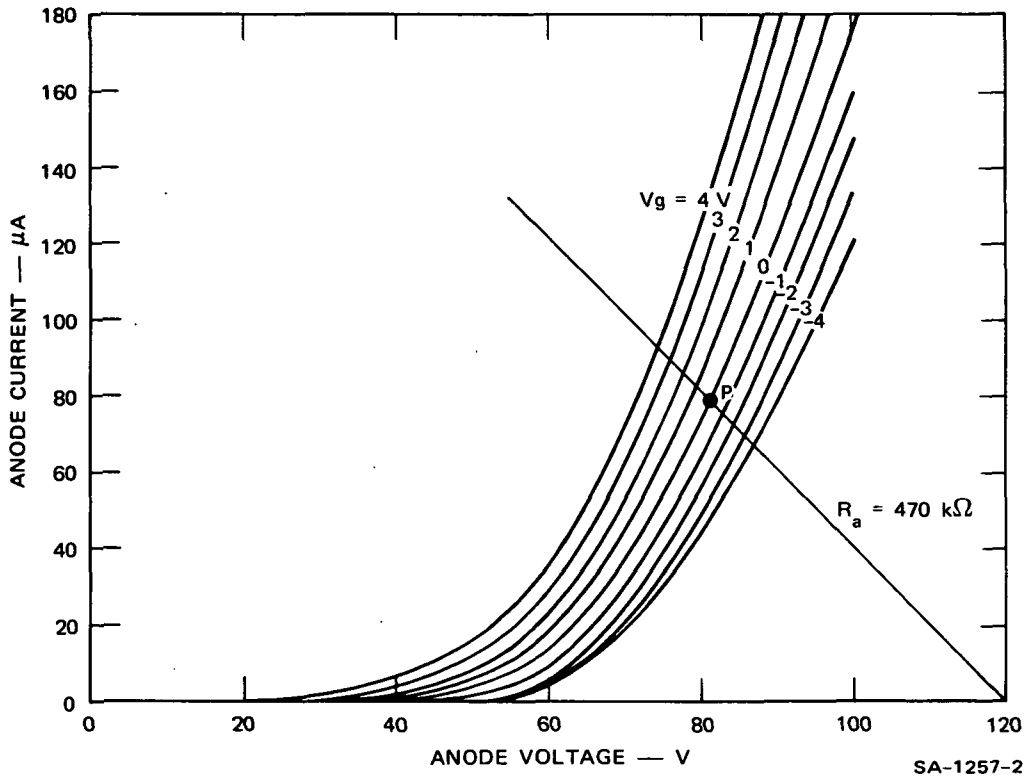

FIGURE 12 I-V CHARACTERISTIC OF TRIODE A, TUBE 16NL

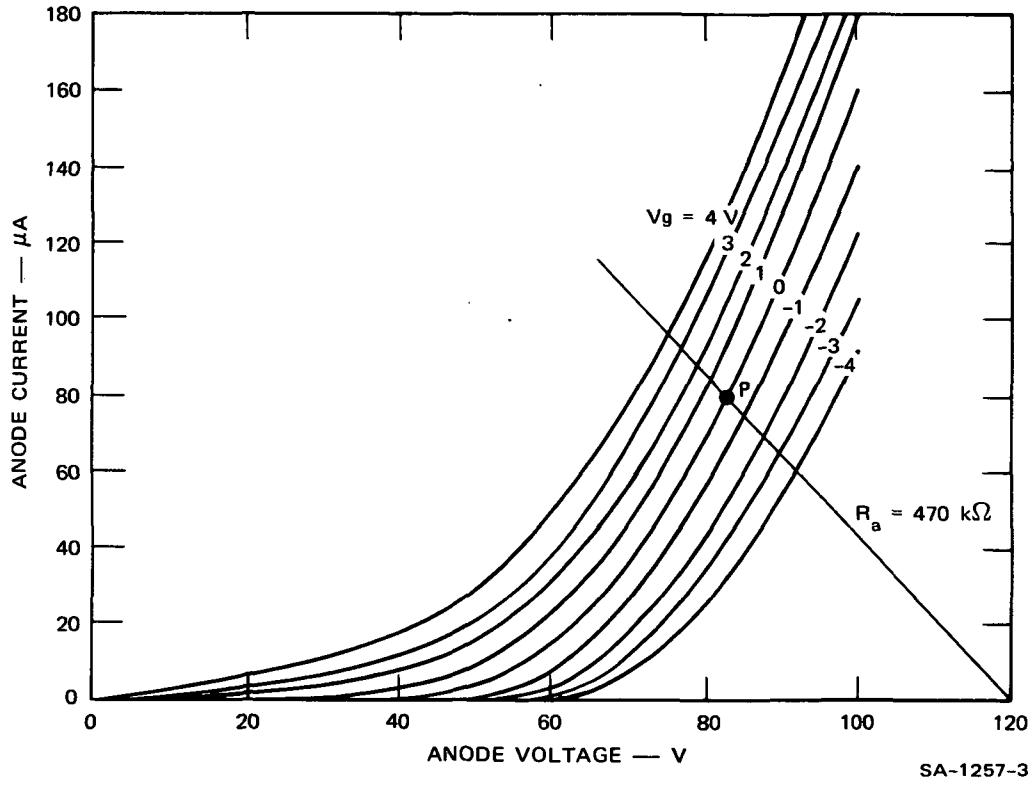

FIGURE 13 I-V CHARACTERISTIC OF TRIODE B, TUBE 16NL

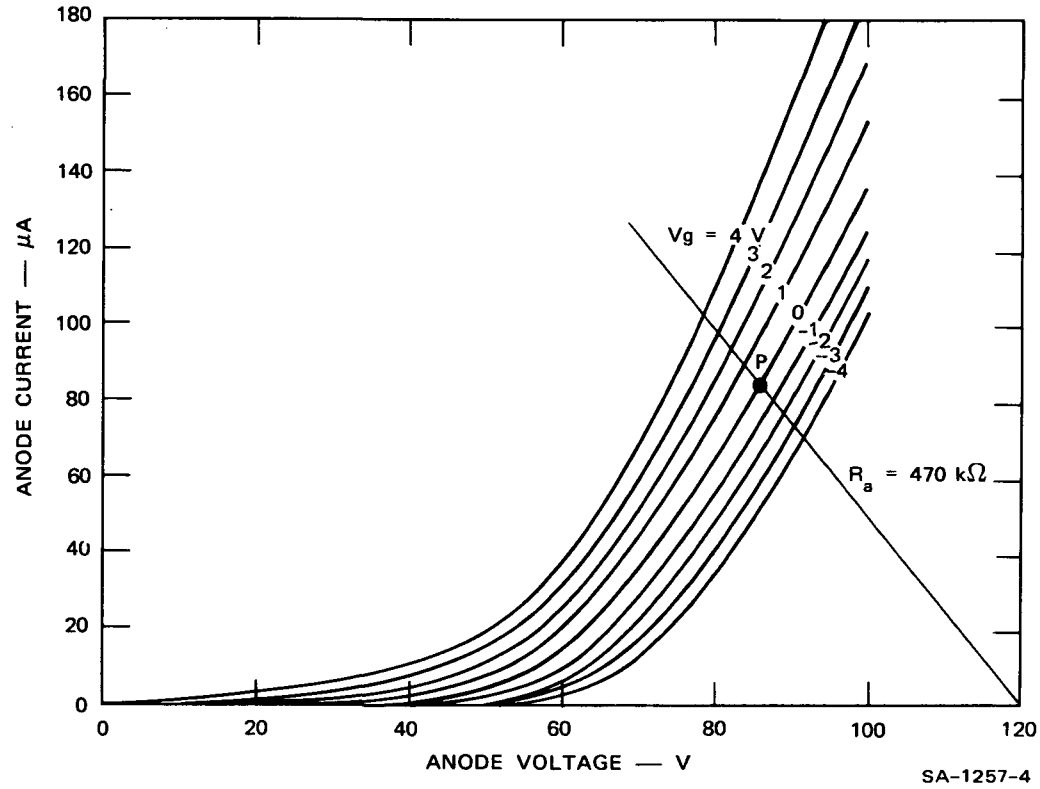

FIGURE 14 I-V CHARACTERISTICS OF TRIODE C, TUBE 16NL

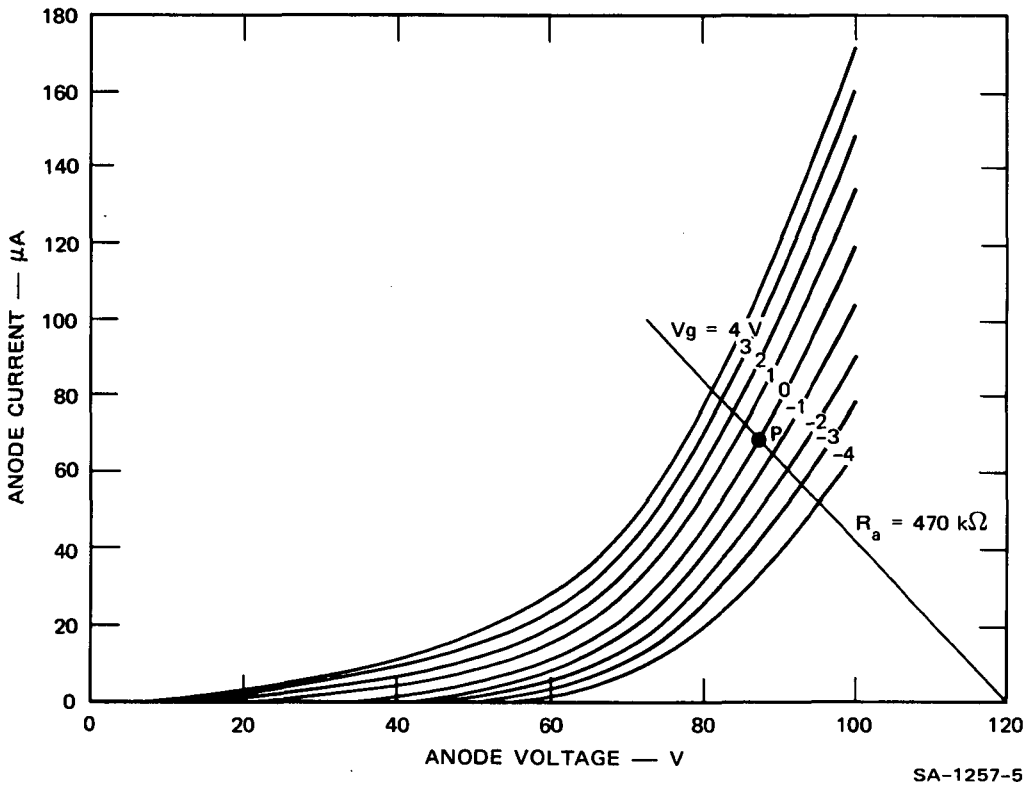

FIGURE 15 I-V CHARACTERISTIC OF TRIODE C, TUBE 21NL

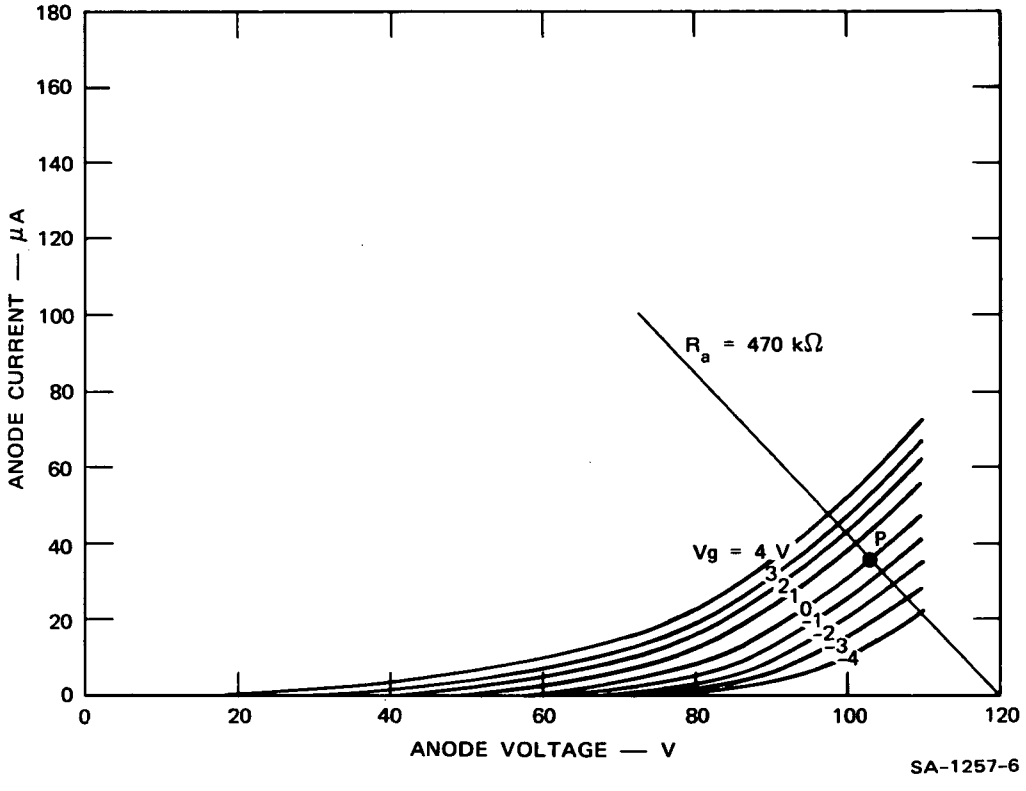

FIGURE 16 I-V CHARACTERISTIC OF TRIODE A, TUBE 21NL

Table IV

AMPLIFICATION FACTOR, μ, AND TRANSCONDUCTANCE, g_m, OF TRIODES

(Anode Voltage = 120 V
Grid Voltage = 0 V
Anode Resistor = 470 kΩ)

Tube No.	Triode	Anode Current μA	Anode Voltage V	μ	g_m, μmhos
16NL	A	80	81	2.5	12
	B	79	83	3.5	13
	C	84	86	3.3	11
20NL	A	95	75	2.5	11
	B	85	80	2.5	9.5
	C*				
21NL	A	69	87	3.0	10
	B	48	97	4.0	10.5
	C	35	103	4.0	6.5

*Accidentally damaged during tests.

the current, voltage, amplification factor, μ, and transconductance, g_m, at the operating point P obtained by biasing the triode with an anode voltage of 120 V through an anode resistor, R_2, of 470 kΩ, and setting the grid potential equal to zero. It should be pointed out that no

attempts were made to optimize μ and g_m, both of which are functions of the geometry of the tube. In a planar triode, the theoretical expression for g_m is given by[7]

$$g_m = \frac{3.51 \times 10^{-6} \left(V_g + \frac{V_o}{\mu} \right)^{\frac{1}{2}} A}{d_{kg}^2 \left[1 + \frac{1}{\mu} \left(\frac{d_{kp}}{d_{kg}} \right)^{4/3} \right]^{3/2}} \text{ mhos} \qquad (2)$$

where V_g and V_o are the grid and anode voltage respectively, A the area of the cathode, d_{kg} the cathode-grid spacing and k_{kp} the cathode-anode spacing. If we use the center-to-center spacing between the thin film electrodes, a cathode area of 2×10^{-3} cm^2, and the data in Table IV we obtain from Eq. (2) a value for g_m close to 200 μmhos. The reason for the low value of g_m is the low current level of the IVC. Using Eq. (1) and (2) we see that g_m is proportional to $J^{1/3} \times A$. Nevertheless, the voltage gain-bandwidth product for an IVC amplifier given by

$$VB \times BW = \frac{g_m}{2\pi C} \qquad (3)$$

is still high, since the output capacitance C associated with the device is very small. VG x BW has previously been estimated to be above 100 MHz.[8]

The amplification factor is basically determined by the distance between the grid and plate electrodes and the width of the grid film. Earlier reported results[1] showed that values of μ close to ten are possible.

The values listed in Table IV indicate that the triode characteristics of tubes 16NL and 20NL are reasonably similar, but that large differences exist among the triodes of tube 21NL, as illustrated in Figures 15 and 16. We have already seen in Figure 9 that the cathode of triode C of tube 21NL is superior to the cathode of triode A, so the poor characteristic of triode C is not associated with poor emission. Essentially, the characteristic of triode C is similar to that of triode A except it has been shifted to a higher anode voltage. We believe that this is due to rapid build up of charge in the substrate because of the high anode voltage.

I. Reverse Emission

In earlier work[2] it was found that triodes with their anodes connected to the cathode of another device exhibited reverse emission; i.e., the triodes were conducting when reversed biased. Since signs of a reaction between the cathode and its connecting film were present, it was suggested that perhaps some of the cathode material had migrated along the metal film to the anode. However, existing data on migration of Ba at high temperatures makes this explanation unlikely. Druzhinin[9] found that barium migration from small orifices in a tungsten foil reached a steady state after 30 minutes at 1300-1400^{o}K, forming circles of a diameter of 90 μm. When slits were used, the distance of migration was reduced to 25 μm. For molybdenum the distances were even less.

A more likely explanation is that the observed reverse emission was due to cross-talk between neighboring devices. In the test circuit of Figure 6, triodes A and B are connected in series so the anode of triode A (anode A) is connected to cathode B. If anode A is made negative with respect to cathode B, cathode B is also negative with respect to cathode A and will, if close enough to cathode A, emit electrons to that cathode. The resulting current, having the appearance of reverse

emission from anode A, should in this case be controllable by the potential of the shield between the two triodes. The results in Figure 17 show that this indeed was the case. Using a small negative potential on the shield, the reverse current of diode A (reverse biased with -30 V on the anode) could be reduced to practically zero. The anode of diode A was composed of grid and anode of triode A connected together to simulate the diodes of the previous program that exhibited reverse emission.

The results indicate that in many cases shielding may be necessary, raising the question as to what degree a negative shield affects the triode characteristics. The effect is illustrated in Figure 18 which shows the characteristic of triode A of tube 16NL when -20 V is applied to the shield. Comparing Figures 12 and 18, we see that the current at anode voltages lower than 60 V has been completely cut off, and that the slope of the curves has decreased, resulting in a movement of the operating point P to a slightly higher current and voltage. A slight reduction of the transconductance from 10 to 9 μmhos is observed, but the amplification factor remains unchanged.

After the turnoff of the shield voltage, it was noticed that the triode characteristic did not immediately return to its original shape. It was particularly noticeable at voltages below 60 V, where the recovery took several minutes. Such an effect could be important in cases where, for example, a triode is turned off by applying a high negative voltage to the grid. Tests were made where -40 V pulses of two to three minutes duration were applied to the grid of triode A biased at the point P. No sign of delay was observed in the switching of the anode current. The triode was also operated as an amplifier with a negative voltage swing on the grid; there was no drop of gain up to about 150 kHz. Thus, the effect of negative voltages appears to be of importance only at small anode voltages.

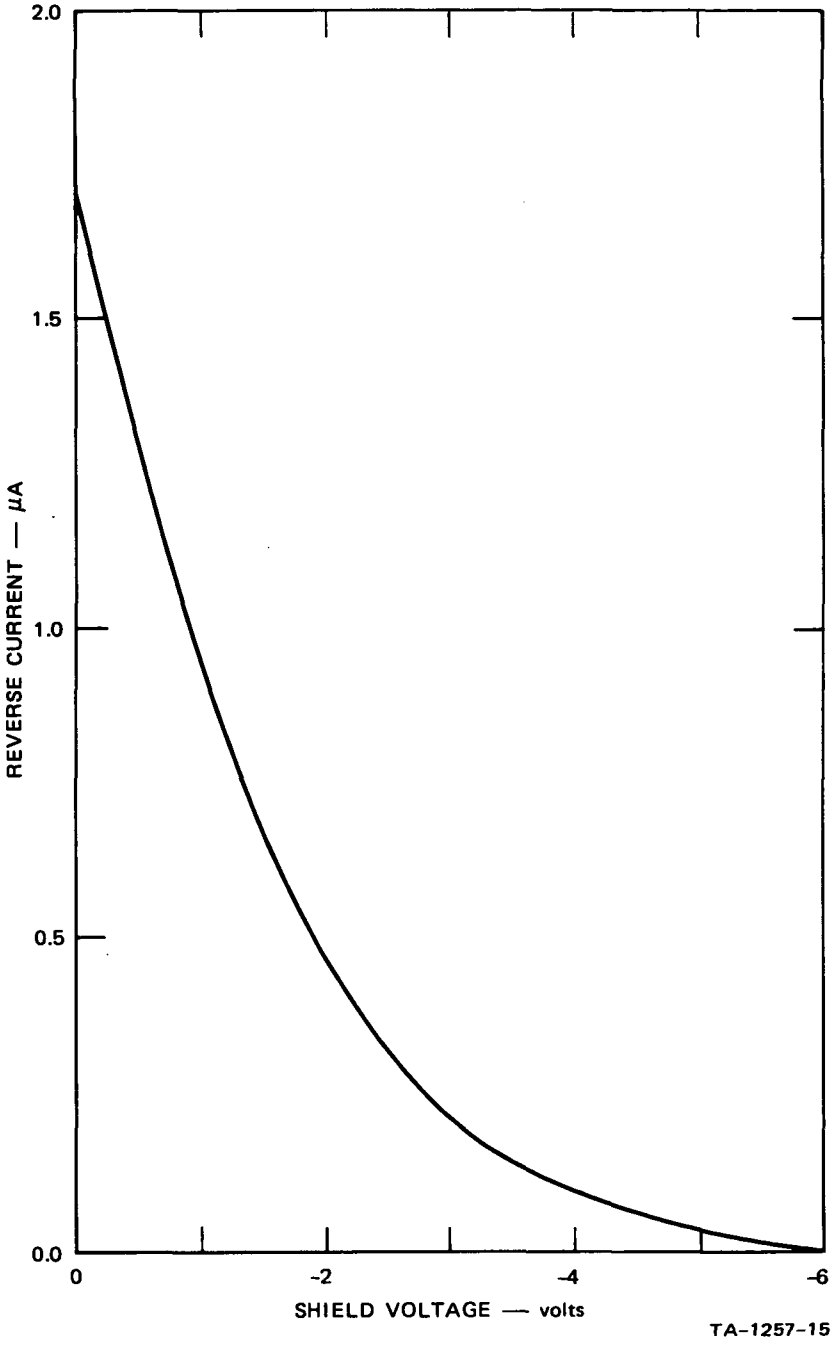

FIGURE 17 REVERSE CURRENT OF DIODE A, TUBE 16NL, AS A FUNCTION OF SHIELD VOLTAGE. Anode voltage was -30 V.

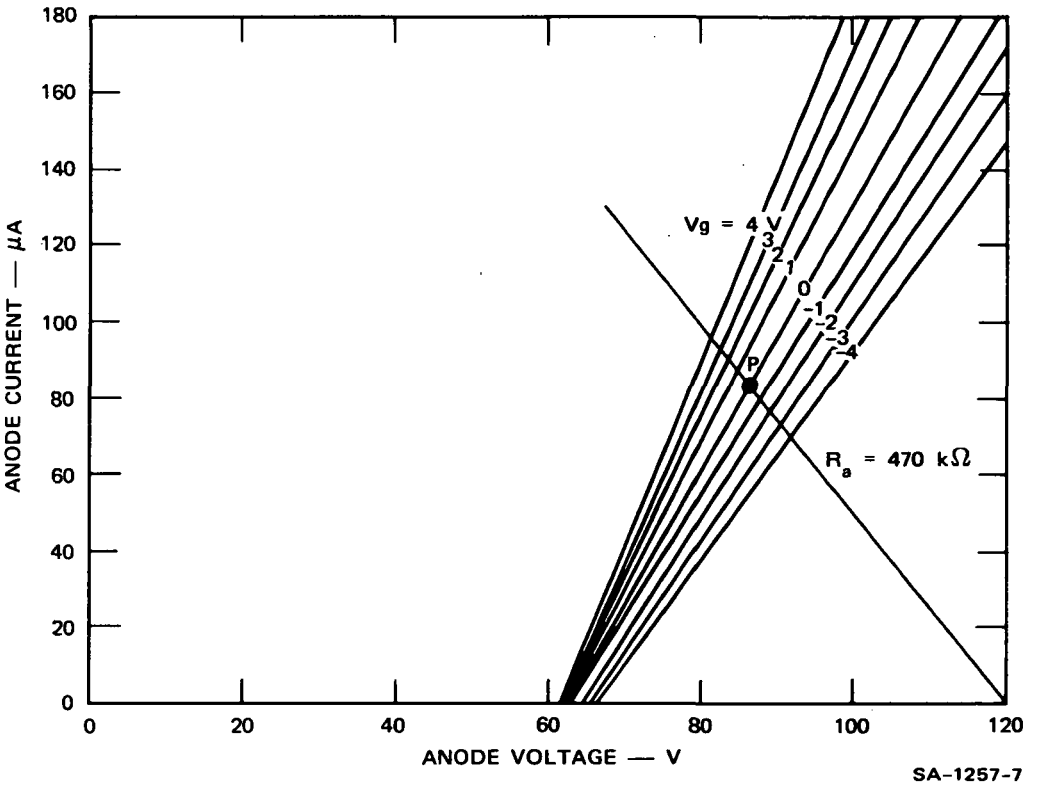

FIGURE 18 I-V CHARACTERISTIC OF TRIODE A, TUBE 16NL, WITH -20 V ON THE SHIELD

J. Effect of Substrate on the Performance of an IVC

In the previous part of this report two cases were described in which application of a voltage to an electrode of the IVC had a persistent effect on the thermionic emission. In all cases the effect eventually disappeared, but the time constant was often of the order of hours. Both polarity and magnitude of the voltage were found to be important. For positive voltages, a fairly high value (100 V) was required, and usually for an extended period of time (hours or days), before any significant effect was noticeable. In contrast, small negative voltages (20 V) had a rapid effect. We will examine these two cases in more detail.

The buildup of space charge in an insulator from an external applied electric field has been known for some time.[10] In the device area it has assumed great significance in the fabrication of MOSFETS (MOS field effect transistors) which for a long time were plagued by buildup of space charge in the SiO_2 at the insulating gate.[11] The problem was eventually solved when the charge mechanism was identified as migration of Na ions in the SiO_2. The devices of the IVC are quite similar to a MOSFET in that the thermionically emitted electrons travel close to the surface of an insulator, the sapphire, and can be greatly affected by any charge on this surface. Some information on the buildup of charge in sapphire does exist. Pyrolytic Al_2O_3 is presently being used as an insulator in MOSFETS for radiation hardened circuits, which has motivated a study of buildup of space charge in this material.[12] A recoverable polarization was observed at all fields, and at fields in excess of 2×10^6 V/cm an electronic current in the sapphire led to trapping of electrons at the electrodes. However, it is questionable whether these results are relevant to our problem since pyrolytic sapphire is polycrystalline and the experiments were performed at

room temperature. Polarization effects have also been observed in single-crystal sapphire irradiated by 30 MeV electrons.[13] A persistent internal polarization was observed similar to the polarization in light-irradiated photoconductors.[14] The results of this investigation are perhaps a little more applicable to our case. The effect of the 30-MeV electrons was essentially to create charge carriers inside the material. This, of course, can also be done by heating the material, as we were doing. Investigation of the electrical conductivity in sapphire at temperatures above 1000°C,[15] performed at SRI a few years ago, showed that single-crystal sapphire acts like a p-type semiconductor with an activation energy of 2.5 eV. A large thermoelectric coefficient indicated that a major part of the conduction may be ionic, in good agreement with studies by Schmalzried[16] that showed that below 1300°C the conduction is both ionic and electronic. With this background information, let us now consider some of the experimental evidence of buildup charges in the sapphire substrate.

Figure 19 shows the decay of a persistent voltage measured between anode and grid of triode C, 21NL, as a result of operating the triode with 100 V on the anode for 2.5 minutes with grid and cathode grounded. The buildup of the persistent voltage for this triode was unusually rapid. Generally, hours were required before the thermionic emission showed any sign of reduction. The voltage was measured with an electrometer while all the IVC electrodes were floating, and was recorded on a strip chart recorder. As Figure 19 shows, a significant positive voltage remained immediately after removal of the 100 V from the anode. It was not possible to measure its initial value because of the time required for making the necessary change of connections to the electrodes and the limited range of the electrometer (10 V). The shape of the curve indicates that the initial value was far in excess of 10 V. More than 15 minutes were required before the potential between the two electrodes reached the

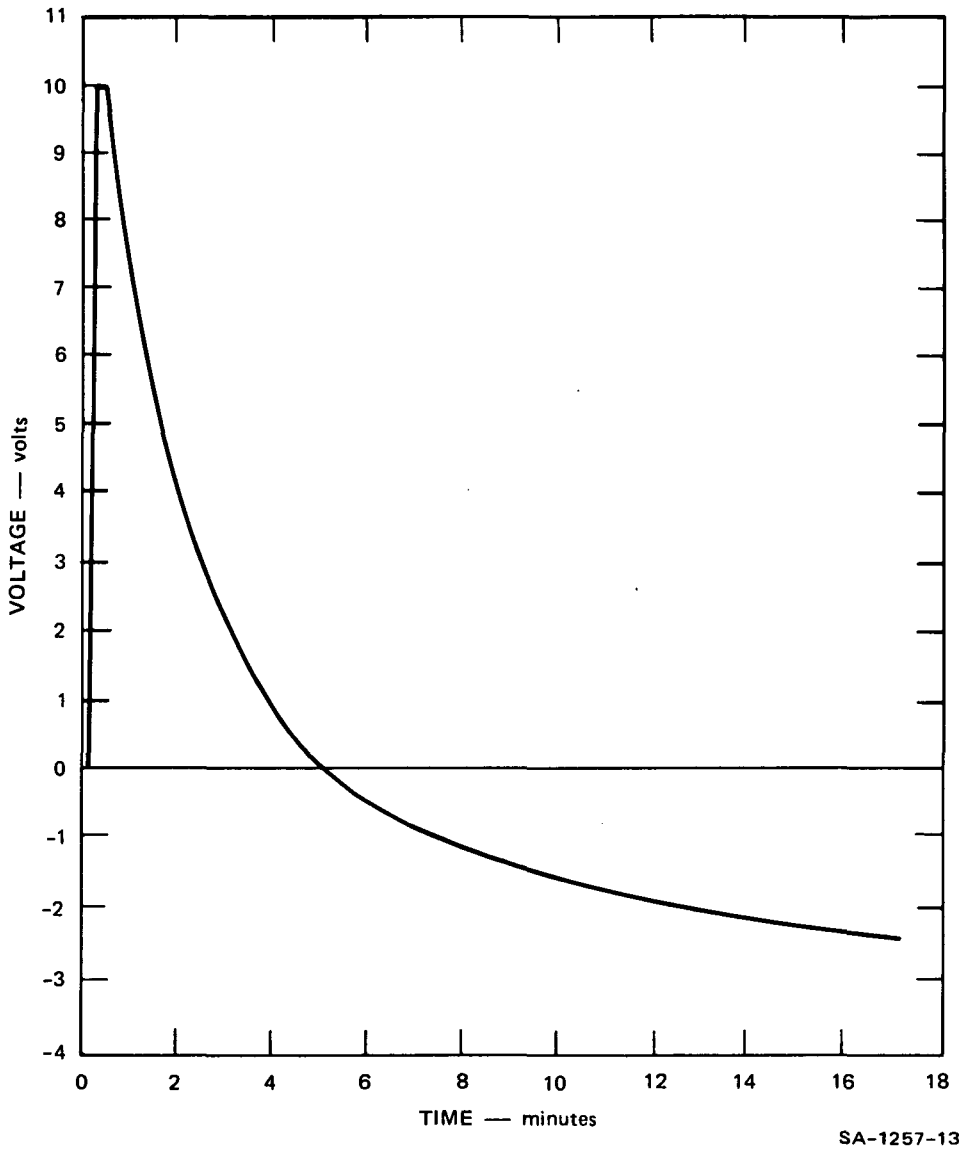

FIGURE 19 DECAY OF VOLTAGE BETWEEN ANODE AND GRID OF TRIODE C, TUBE 21NL. The curve was measured immediately after removal of 100 V which was applied between the two electrodes for 2.5 minutes.

steady-state value of -3.2 V, determined by the position of the electrodes relative to the potential distribution of the heater strip underneath the wafer.

Figure 20 illustrates a possible charge distribution built up in the sapphire as a result of application of a high voltage on the anode. In agreement with observation of polarization in insulators, we have negative charge at the positive electrode and positive charge at the negative electrode. The shape of the charge distribution in Figure 20 is exaggerated to illustrate that we expect most charges to be at the edges of the electrodes where high fields exist. Also, we have assumed that the charge distribution extends beyond the electrodes and is not merely limited to the surface. The last two assumptions are important, because the charge directly underneath the electrodes and the positive charge at the surface neutralized by electrons have little or no effect on the electric field in vacuum between the electrodes. However, positive charge trapped below the surface of the sapphire and located just beyond the edge of the electrodes forms, with its neutralizing electrons on the surface, dipoles that do affect the electric field at the edge of the electrode. Since most of the current presumably comes from or is collected by areas in close vicinity to the edges, the stray field of the dipoles in this region could have a significant effect. We have shown no surface neutralization of the negative charge in Figure 20. Undoubtedly, positive ions are present on the surface of the sapphire, but we expect their number to be too small to provide complete neutralization. If a large fraction of the negative charge in front of the anode is not neutralized, a sharp voltage drop exists in this area, causing the triode characteristics to shift to higher anode voltages, as we saw in Figure 16 for the case of triode C, 21NL, where the shift was unusually high.

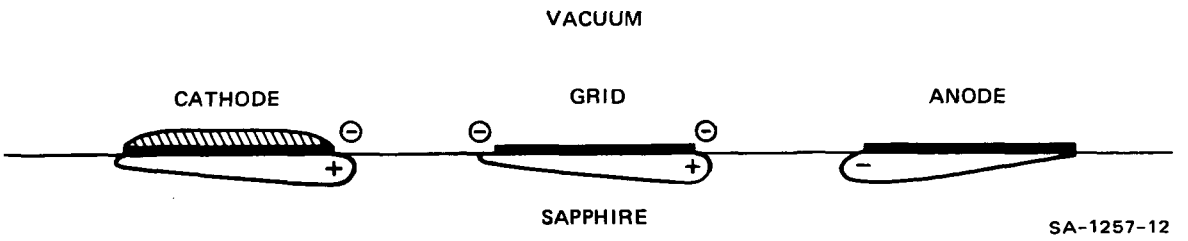

FIGURE 20 ILLUSTRATION OF A POSSIBLE CHARGE DISTRIBUTION IN SAPPHIRE. The space charge is caused by a high positive voltage (100 V) on the anode.

To get a better understanding of this phenomenon, the three triodes of tube 21NL were compared; it was found that the magnitude of the persistent voltage built up between anode and grid during the operation of the triodes was reflected in the magnitude of the shift of the triode characteristics along the axis of anode voltage. A large persistent voltage corresponded to a large shift to higher voltages. Studying the barrier between the anode and sapphire, a similar correspondence was observed. A large barrier always led to a higher persistent voltage. The anode-sapphire barrier for the triodes of tube 16NL showed little variation, in good agreement with the small differences between triode characteristics of this tube. Thus, two processes appear to take place, one with a time constant short enough to affect the measured triode characteristics, and one with a long time constant affecting the long-term stability of the triodes.

The charge distribution shown in Figure 20 predicts that the potential of the grid with respect to the cathode should be negative, which indeed was measured. The presence of dipoles at the edges of the cathode may explain the added retarding potential observed in Figure 11. This potential not only affects the diode characteristic but also influences the triode

characteristic. Since the current in a triode is proportional to $(V_g + V_a/\mu)^{3/2}$, where V_g and V_a are the grid and anode potential respectively, and μ is the amplification factor, any increase of the retarding potential between grid and cathode results in a shift of the triode characteristic that is μ times the increase. The shift of the triode characteristic is thus a combined effect associated with accumulation of charge at both cathode and anode, and may explain the occurrence of two time constants.

The effect of applying a small negative potential to an electrode has already been illustrated in Figure 18, which shows the effect of -20 V on the shield on the triode characteristic. In Figure 21, we have shown the recovery of diode A, 16 NL, after -20 V was applied to the shield

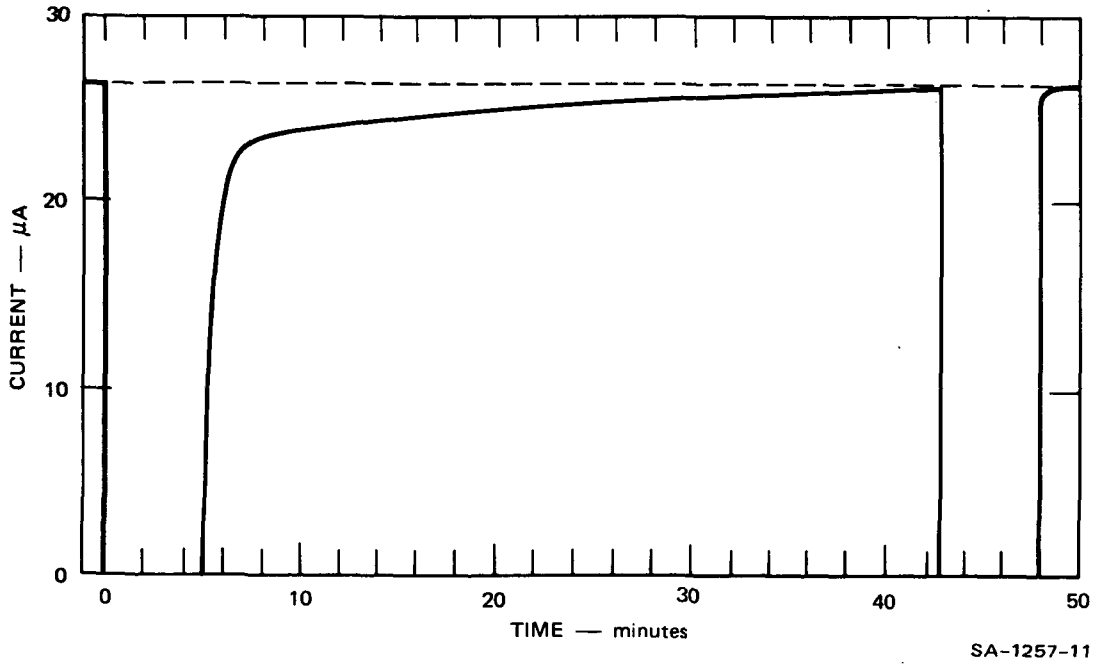

FIGURE 21 RECOVERY OF CURRENT OF DIODE A, TUBE 16NL. The recovery was measured after -20 V was applied to the shield for five minutes during which period the diode voltage of 10 V was turned off. Also shown is the on-off response of the diode at the end of the recovery period.

for five minutes, during which time the diode was disconnected. When the diode was switched on again, the current rose to about 90% of its final value within approximately one minute, after which the recovery slowed significantly, premitting full recovery after about 45 minutes. For comparison, Figure 21 also shows the on-off response of the diode when it had almost completely recovered. In the latter case, the response time was governed entirely by the recorder. Application of +20 V to the shield showed no persistent effect on the diode current.

The most obvious explanation for the difference between the effect of the two polarities is that the negative potential on an electrode creates trapped negative charges at the grounded cathodes. Since the negative charge is only partly neutralized by positive ions, it has a much stronger effect on the thermionic emission than the dipoles created by positive voltages.

We have so far been concerned only with the effect of charges trapped in the substrate, ignoring the effect of ions except for possible neutralization of trapped negative charge at the sapphire surface by positive ions. A variety of ions are undoubtedly present on the surface of the sapphire from the etching processes, and the relatively impure Grafoil heater may also act as a source of ions at high temperatures. Since Grafoil has the added disadvantage of outgassing quite strongly during activation, it was decided to attempt to replace it by a pure metal heater and at the same time observe any effect that such a change might have on the persistent effects described above. Metal heater strips were etched out of one-mil foils of Mo and W. In all cases the use of these heaters led to nonuniform heating of the wafer because of variations in the thermal contact between heater and wafer. Grafoil is better than metal in this respect because of its greater ductility. No improvement with respect to persistent effects was observed.

A closer examination of the effect of surface polarization due to

ions indicates that it cannot explain all our observations. For example, in the case illustrated in Figure 20, the presence of positive ions at the cathode and grid would have no effect on the diode formed by grid and cathode because the positive ions would be neutralized by electrons. That we definitely are dealing with other effects than just ion migration on the surface is suggested by the fact that the current of a diode not only depends on the voltage between grid and cathode but also on the polarity of the cathode with respect to the heater strip. Consider the experiment consisting of measuring the current of a diode formed by grid and cathode of a triode, first with +10 V on the grid and with the cathode grounded, then with -10 V on the cathode and with the grid grounded. The electric field between the two electrodes and any possible effect from ions on the surface should be identical in the two cases. However, the diode current was always 20% to 30% smaller when -10 V was applied to the cathode. The explanation for this discrepancy, we believe, is associated with a large leakage current (several nA) to the heater which was always present when an electrode was negatively biased. The leakage current was about one order of magnitude higher than that obtained for a comparable positive voltage. The large leakage current may have facilitated the accumulation of charges at the cathode, reducing the diode current.

To see to what degree the persistent effect described above was solely a characteristic of sapphire, a few experiments were made in which sapphire was replaced by spinel ($MgAl_2O_4$). Similar time-varying anode currents were observed, and since at the same time the outgassing of spinel was severe during activation and its resistivity at 700^{o} was too low, experiments with spinel were abandoned.

It is quite clear that more work is needed before a complete understanding can be obtained of the effect of trapped charges in the substrate on the flow of electrons between the electrodes of an IVC. The test

circuit we were using in the experiments was not designed for this purpose. Simpler circuits are needed so that good estimates of the current and field distribution can be obtained. A factor that complicated the investigation greatly was the long time constant of some of the effects and the fact that the charge distribution in the sapphire was frozen in when the wafer was cooled to room temperature. This made it necessary to keep close track of past experiments performed on each wafer in order to interprete the data which otherwise would have appeared inconsistent.

In the study of the persistent polarization of sapphire irradiated by high-energy electrons[13] it was found that the polarization depended on the nature of the sapphire surface and the contact attachment techniques. This is in agreement with our observation of the importance of the barrier between the anode and the sapphire. Thus, changes of the surface preparation of the sapphire and the method of thin film deposition may eliminate the problems that at the moment are limiting the performance of the IVC.

V RECOMMENDATIONS

Any future program must be directed toward solution of the problem of trapped charges in the substrate. A better understanding is needed not only of the nature of the polarization of the sapphire but also of the flow of electrons in vacuum between the electrodes. This will help the evaluation of the effect of stray electric fields from charges in the substrate and will also provide the tools necessary for evaluation of the effect of the electrode configuration on the device characteristics. The range of values of amplification factor and transconductance that can be obtained using the various device structures should be estimated and evaluated in terms of practical circuits that can be built using those values. Also, estimates should be made of the maximum packing density of circuit elements that can be obtained on the substrate, considering such factors as cross-talk and the area needed for capacitors.

ACKNOWLEDGMENTS

The author would like to thank A. Fripp, NASA, Langley Research Center, for many useful discussions and for the photomicrograph shown in Figure 7. Thanks are also due to F. A. Halden, P. J. Jorgensen, S. R. Morrison, and D. Nitzan for many helpful comments and suggestions, to J. H. Hunt and D. Murdock for fabrication of the devices, and to R. B. Yeaton, Superior Tube Company, Norristown, Pennsylvania, for providing a foil of Cathaloy A-31.

REFERENCES

1. R. A. Kjar and J. E. Bell, "Characteristics of MOS Circuits for Radiation-Hardened Aerospace Systems," IEEE Trans. on Nuclear Science, NS-18, 258, 1971

2. A. Rosengreen and D. Nitzan, "Low-Temperature Thermionic Emitter," Final Report, NASA Contract NAS 12-607, SRI Project No. 7147, Stanford Research Institute, May 15, 1970

3. D. V. Geppert, B. V. Dore, and R. A. Mueller, "Low Temperature Thermionic Emitter," Interim Scientific Report, NASA Contract NAS 12-607, SRI Project No. 7147, Stanford Research Institute, May 19, 1969

4. E. S. Rittner, "A Theoretical Study of the Chemistry of the Oxide Cathode," Philips Res. Rep. 8, 184, 1953

5. G. H. Metson, "Platinum-cored Thermionic Valves in the Transatlantic Telephone Cable," Platinum Metal Rev. 2, 2, 1958

6. W. H.Kohl, "Handbook of Materials and Techniques for Vacuum Devices," Reinhold Publishing Corporation, New York, 1967

7. J. W. Gewartowski and H. A.Watson, "Principles of Electron Tubes," D. Van Nostrand Company, Inc., New York, 1965

8. B. V. Dore and R. A. Mueller, "Low Temperature Thermionic Emitter," Quarterly Report No. 5, NASA Contract NAS 12-607, SRI Project No. 7147, Stanford Research Institute, Nov. 15, 1969

9. A. V. Druzhinin, "Barium Migration on Tungsten, Molybdenum and Rhenium Surfaces Covered with an Adsorbed Gas Film," Radio Engineering and Electronic Physics, 10, 425, 1965

10. A. R. von Hippel, "Dielectrics and Waves," John Wiley & Sons, Inc., New York, 1954

11. E. H. Snow and B. E. Deal, "Polarization Effects in Insulating Films on Silicon--A Review," Trans. Metal Soc. AIME, 242, 512, 1968

12. R. H. Walden and R. J. Strain, "Conduction in Films of Pyrolytic Al_2O_3," 8th Annual Proceedings Reliability Physics, Las Vegas, Nevada, April 7-10, 1970

REFERENCES (Concluded)

13. J. W. Harrity and R. E. Leadon, "Polarization Effects in Irradiated Single-Crystal Sapphire," Conference on Electrical Insulation and Dielectric Phenomena, National Academy of Sciences, Washington, D.C., 1969

14. J. R. Freeman, H. P. Kallmann, and M. Silver, "Persistent Internal Polarization," Revs. Modern Phys. 33, 553, 1961

15. L. Feinstein, et al., "Research on Dielectrics for Microwave Electron Devices," Final Report, Contract DA28-043 AMC-00215(E), Stanford Research Institute, February 1966

16. H. Schmalzried, Z. Physik Chem. 38, 87, 1963.

NASA CR-112108

DISTRIBUTION LIST
NAS1-10815

	No. Copies
NASA Langley Research Center Hampton, VA 23365	
Attn: 122/Acquilla D. Saunders	1
115/Raymond L. Zavasky	1
470/Archibald L. Fripp, Jr.	25
NASA Ames Research Center Moffett Field, CA 94035	
Attn: 202-3/Library	1
213-3/Thomas B. Fryer	2
NASA Flight Research Center P. O. Box 273 Edwards, CA 93523	
Attn: Library	1
Donald W. Veatch	2
Goddard Space Flight Center Greenbelt, MD 20771	
Attn: Library	1
711/David H. Schaefer	1
NASA Manned Spacecraft Center 2101 Webster Seabrook Road Houston, TX 77058	
Attn: JM6/Library	1
EB7/Saverio Gaudiano	1
NASA Marshall Space Flight Center Huntsville, AL 35812	
Attn: Library	1
S&E-ASTR-RM/Dorrance L. Anderson	1
S&E-ASTR-RS/Dr. Alvis M. Holladay	1
Jet Propulsion Laboratory 4800 Oak Grove Drive Pasadena, CA 91103	
Attn: 111-113/Library	1
NASA John F. Kennedy Space Center Kennedy Space Center, FL 32899	
Attn: IS-DOC-12L/Library	1
NASA Lewis Research Center 21000 Brookpark Road Cleveland, OH 44135	
Attn: 60-3/Library	1
77-1/John Shirman	2

NASA CR-112108

DISTRIBUTION LIST
NAS1-10815

	No. Copies
National Aeronautics & Space Administration Washington, DC 20546	
Attn: KSS-10/Library	1
REE/Dr. Bernard Rubin	3
REE/Charles E. Pontious	3
Department of Defense Advisory Group on Electron Devices 201 Varick Street, 9th Floor New York, NY 10014	
Attn: D. Klieger	5
Laboratory for Physical Sciences 4928 College Avenue College Park, MD 20740	
Attn: Dr. E. Burke	1
Wright-Patterson Air Force Base, OH 45433	
Attn: Gene Maupin, AFAL/NVE	1
Navy Air Systems Command Jefferson Plaza Washington, DC 20360	
Attn: James Fox, AIR 52022	1
IIT Research Institute 10 West 35th Street Chicago, IL 60616	
Attn: Harold A. Lauffenburger, Program Manager Reliability Analysis	1
NASA Scientific & Technical Information Facility P. O. Box 33 College Park, MD 20740	14 plus reproducible